# Brosilow-Ziff model for the CO-NO surface reaction on disordered two- and three-dimensional substrates

Joaquín Cortés* and Eliana Valencia
*Facultad de Ciencias Físicas y Matemáticas, Universidad de Chile, P.O. Box 2777, Santiago, Chile*
(Received 23 December 2002; published 11 July 2003)

The Brosilow-Ziff model, which for a uniform lattice shows superficial poisoning by the ''checkerboard mechanism'' for simplified Langmuir-Hinshelwood kinetics of the reduction reaction of NO by CO, has been studied in the case of various disordered substrates: two-dimensional (2D) incipient percolation cluster, backbone, and diffusion-limited aggregate (2D) fractals, together with a deterministic fractal and a statistical substrate, both three-dimensional. Some additional effects such as diffusion, nearest-next-neighbor sites, and desorption are also considered. The systems were found to be nonreactive and pseudoreactive in all the cases which showed the checkerboard mechanism. Otherwise, a reactive zone (window) related directly to the geometric structure of the substrate is seen.

DOI: 10.1103/PhysRevE.68.016111 PACS number(s): 05.70.−a

## I. INTRODUCTION

During recent decades there has been considerable interest in irreversible dynamics systems that exhibit complicated behaviors, including dissipative structures, fluctuations and oscillations, irreversible phase transitions (IPTs), etc. [1]. The behavior of these far-from-equilibrium many-particle systems is a challenge in many branches of science such as physics, chemistry, biology, ecology, and even sociology.

Surface reactions under flow conditions are good examples of those nonequilibrium systems, which are also of interest in real catalysis problems. The studies of IPTs of those systems have been reviewed very well by Evans [2], Zhdanov [3], and Albano [4]. Even though it has been possible to clarify a number of phenomena observed in the laboratory, such as poisoned and reactive zones, bifurcations, etc., the complexity of these systems has made it difficult to check experimentally the highly interesting theoretical advances that have been confirmed only through computer simulations. The latter have become powerful tools, particularly since Ziff *et al.* [5] studied the catalytic oxidation of CO on a square lattice and found irreversible phase transitions on the surface (the ZGB model).

The study of the monomer-dimer (MD) reaction of type $A+B_2$, which mimics the $CO+O_2$ reaction, analyzed by means of the ZGB model, was followed by many papers in which various authors have studied, from different points of view, a large number of other systems such as, for example, monomer-monomer (MM) [5,6], dimer-dimer (DD) [7], monomer-trimer (MT) [8], dimer-trimer (DT) [8,9], or the MD-type $A+BC$ model [10–14], which mimics the reduction of NO by CO.

In general, in the case of systems formed by catalytic surface reactions, the difficulties for interpreting the system are related to the knowledge of the reaction mechanism and to the characteristics of the substrate acting as a catalyst. Although most of the papers assume a uniform catalytic surface that can be associated with a catalyst formed by a single crystal, for some time interest has extended to the study of disordered surfaces modeled through fractals, for example, motivated by the fact that most of the catalysts are made up of tiny clusters of metal particles dispersed in an inert support. Such is the case of the studies of random fractals such as percolation clusters by Albano [4,15], Casties *et al.* [16], Hovi *et al.* [17], and our group [18], or of diffusion-limited aggregates (DLA) [19] and deterministic fractals such as the Sierpinski carpet and gasket [20].

In most of these papers, however, the substrate has been modeled by means of a two- dimensional fractal, and only recently have three-dimensional fractal surfaces been considered [21–23]. This is, among others, one of the aspects that we are interested in studying in this paper, analyzing a classical model of the MD-type $A+BC$ reaction. Our motivation has to do with the characteristics of that simple model related to the system's reactivity and with the interest that the reduction reaction of NO by CO (CO-NO reaction) has from both the theoretical and experimental viewpoints, due to the controversies that still exist around its kinetic mechanism. Also, together with the CO oxidation reaction, this reaction is important in automotive exhaust emission control.

## II. MODEL AND SIMULATION

### A. Surface reaction model

The mechanism of the $CO+NO$ reaction on noble metal catalysts, especially on Rh catalysts, has been extensively investigated since the early 1980s [24]. The most recent work shows that the discussion of this reaction is far from exhausted; for example, the way in which $N_2O$ participates in the system's mechanism is still a matter of controversy. Moreover, a new mechanism for a supported catalyst, which has not yet been studied in detail, was proposed recently [25] and was considered in one of our recent experimental papers [26], distinguishing it from the one that describes the behavior of the reaction on a single crystal.

Considering mechanisms under various assumptions and degrees of simplification, this reaction was simulated origi-

*Electronic address: jcortes@dqb.uchile.cl

 

nally on a uniform surface by means of Monte Carlo (MC) mathematical experiments by Yaldram and Khan [12,27]. It was later analyzed by Brosilow and Ziff (BZ) [10] and by Meng, Weinberg, and Evans (MWE) [11,28], and was then studied by our group through MC simulations [29] and field models [13], and by Dickman [14].

A very interesting argument given by BZ [10] and analyzed later by MWE [11] shows that the system leads inevitably to its poisoning by a process of ''checkerboarding'' of $N(a)$ atoms if a two-dimensional and uniform square catalytic lattice and the following simplified Langmuir- Hinshelwood (LH) mechanism are assumed for the reaction:

$$CO(g)+E \xrightarrow{y_{CO}} CO(a), \tag{1}$$

$$NO(g)+2E \xrightarrow{y_{NO}} N(a)+O(a), \tag{2}$$

$$CO(a)+O(a) \xrightarrow{k_1} CO_2(g)+2E, \tag{3}$$

$$N(a)+N(a) \xrightarrow{k_2} N_2(g)+2E. \tag{4}$$

Here $(g)$ denotes gas-phase species, $(a)$ denotes adsorbed species, and an empty site on the surface is denoted by $E$.

A reactive window is seen in some part of the phase diagram if one considers a mechanism which, beside steps (1)–(4) above, includes additional reactions or considers other coordinations of the superficial sites, as has been analyzed by MWE [11] and our group [29] in the case of uniform surfaces. The BZ mechanism had not been studied, however, in the case of disordered substrates such as fractals, which are closer to most experimental catalysts. It is for these reasons that in this paper we have studied the case of some substrates made of two-dimensional fractals such as the incipient percolation cluster (IPC), the IPC backbone, and diffusion-limited aggregation (DLA). We also consider some substrates which in this paper we have called three-dimensional objects to indicate two-dimensional surfaces that extend over three dimensions like a rough surface, such as a statistical disordered substrate that we shall call DLA3X, and a deterministic fractal that we shall call FRX, the latter generated from a set of affine transformations. Conventionally we are denoting by DLA3X a substrate constructed using the DLA(3D) fractal as a base, and by FRX the deterministic fractal generated from autosimilar structures as described in the Appendix.

### B. Simulations

The figures show the phase diagrams of the systems studied in this paper, corresponding to the fractions of covered surface of the different adsorbates and the $CO_2$ production versus CO concentration in the gas phase, $y_{CO}$, obtained by MC simulations in agreement with the mechanism given by Eqs. (1)–(4) over various substrates generated as described in the Appendix, where details of the generation of the active sites and some other aspects are given. Some simulations include the possibility of desorption or diffusion. The probability of desorption is measured by the adsorption/desorption $(A/D)$ ratio. A ratio of $A/D=1/j$ means that the probability for a desorption event is $j$ times larger than for an adsorption event. The probability of diffusion is determined in a similar way.

The impingement rate for $CO(g)$ is denoted by $y_{CO}$, and that for $NO(g)$ by $y_{NO}$. These are normalized so that $y_{CO}+y_{NO}=1$. Reactions between neighboring $CO(a)$ and $O(a)$ and between neighboring $N(a)$ occur instantaneously (i.e., $k_1=k_2=\infty$). The details of the MC simulations are in general the same that we have explained previously [13,18,29]. In this case we consider a lattice of active sites without periodic boundary conditions which simulate in each case the corresponding catalytic substrate.

Simulation starts with a clean substrate. The steps involved in the simulation procedure are as follows: at each simulation step a substrate site is chosen randomly, and then it is decided via random numbers whether an adsorption, diffusion, or desorption step will be performed next.

If an adsorption process is required, the chosen site is examined and, if it is already occupied, the event is rejected and the trial ends; if it is vacant, whether the molecule will be CO with a probability $y_{CO}$ or NO with a probability $y_{NO}$ is chosen randomly. A CO molecule is adsorbed immediately if the site is vacant, but the NO molecule needs two vacant nearest-neighbor (NN) sites to be adsorbed, so one of the possible directions (four in 2D and six in 3D for the DLA3X substrate) is chosen randomly, and if the neighbor determined by that direction belongs to the fractal and is empty, the molecule is adsorbed, otherwise the event is rejected and the trial ends.

The reaction step is analyzed immediately in the case of a successful adsorption. If the adsorbed molecule is CO, all the neighbors to be considered are scanned for the presence of an O atom. If O atoms are found, one of them is randomly chosen to react with CO through reaction step (3) and the trial ends. In the case of a successful adsorption of NO, the neighbor sites of $N(a)$ and $O(a)$ atoms are then examined randomly (as discussed above) for the presence of $N(a)$ or $CO(a)$ in order to complete reaction steps (4) and (3), respectively. Thus, when $CO_2$ or $N_2$ molecules are produced, they are instantaneously desorbed from the surface, leaving behind two vacant sites. In the two-dimensional fractals the number of neighbors to consider is four, except when there are diagonal actions, in which case eight neighbors are considered, all with equal weight.

If the process of desorption of the CO molecules has been chosen, the selected site is examined for occupancy by a CO molecule, and if that is the case the molecule is desorbed, leaving the site vacant, otherwise the event ends. In those cases in which diffusion of CO is considered and this event is selected, if the randomly chosen site contains CO, a NN of the lattice sites is selected randomly, and if it belongs to the fractal and is vacant, the CO molecule is transferred to that site, otherwise the event ends.

For the processes on the three-dimensional DLA3X substrate (see the Appendix), a cubic element of the DLA(3D) fractal that serves as the basis is chosen randomly and then a site $S_1$, located on one of the exposed faces of the selected

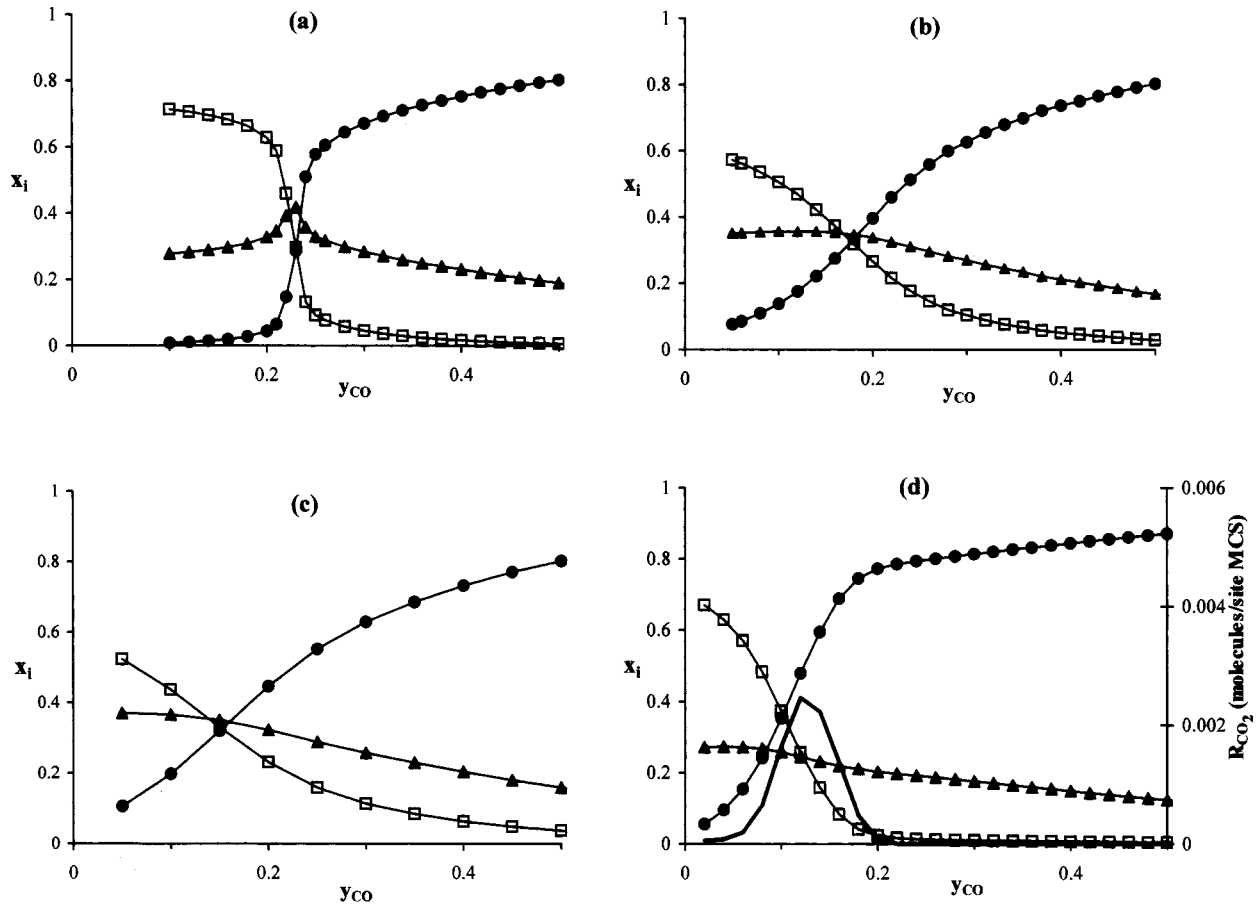


FIG. 1. Variation of steady state of the coverage $x_i$: $x_{CO}$(●), $x_O$(□), $x_N$(▲), as a function of the impingement rate for CO($g$), $y_{CO}$ (phase diagram), obtained by MC for the CO-NO reaction and the LH mechanism (1)–(4). (a) On the uniform substrate. (b) On IPC. (c) On DLA (2D) for NN coordination of superficial sites. (d) The same as (c) but for NNN site coordination in the reaction steps; production rates of $CO_2$, $R_{CO_2}$ (——) (in the coverage curves the lines have been drawn to guide the eyes).

element, is chosen randomly. Once site $S_1$ has been chosen, the corresponding adsorption, reaction, diffusion, or desorption processes are carried out as appropriate. For the NO adsorption process, for example, a site $S_2$ is chosen next to an $S_1$ among the five possible ones [the direction toward the DLA(3D) fractal is excluded]. If $S_1$ and $S_2$ are located on exposed faces of the fractal and they are vacant, adsorption occurs. In the case of the reaction, which occurs immediately after a successful adsorption, if there are no diagonal actions the surroundings of the particle just adsorbed are revised randomly in the six directions, and if there are diagonal actions, the 12 closest diagonal neighbors are added to the surroundings. If there are two neighbors that can react, they do so, leaving two vacant sites.

The simulation of these processes on the FRX fractal is done in a similar way, taking into account that in this case the number of neighbors can be different for each fractal site as described in the Appendix. In the NO adsorption step, for example, once it is shown that the first site chosen is empty, one of its neighbors is chosen randomly, and if it is empty, the molecule is adsorbed at the two sites.

Even though in this work no sensitivity studies have been made concerning finite size effects, from our experience in the case of two-dimensional fractals and from what appears in the literature in relation to FRX and DLA fractals for the rest of the substrates, the sizes of the substrates have been chosen so that they adequately guarantee the reproducibility of the results for the processes developed in the paper.

## III. RESULTS AND DISCUSSION

Figure 1 shows the phase diagrams of the CO-NO reaction according to reaction mechanism (1)–(4) for some two-dimensional substrates. Figure 1(a) shows the well-known case of a uniform surface on which the system has no reactive steady state because of the checkerboard structure that is formed on the surface. The same absorbent situation is seen in Figs. 1(b) and 1(c), where reaction occurs on the IPC and DLA(2D) fractals, respectively. We have not included the case of another fractal, the IPC backbone (see the Appendix), because its phase diagrams are practically identical to that of the IPC. This indicates that suppression of the hanging branches of the IPC [30] connected to the bone in its structure does not affect the behavior of the CO-NO reaction. In Fig. 2, which shows the phase diagrams of the same system on some three-dimensional substrates, we can see two other cases without a reactive steady state, corresponding to DLA3X without diffusion [Fig. 2(a)] and with diffusion [Fig. 2(c)].

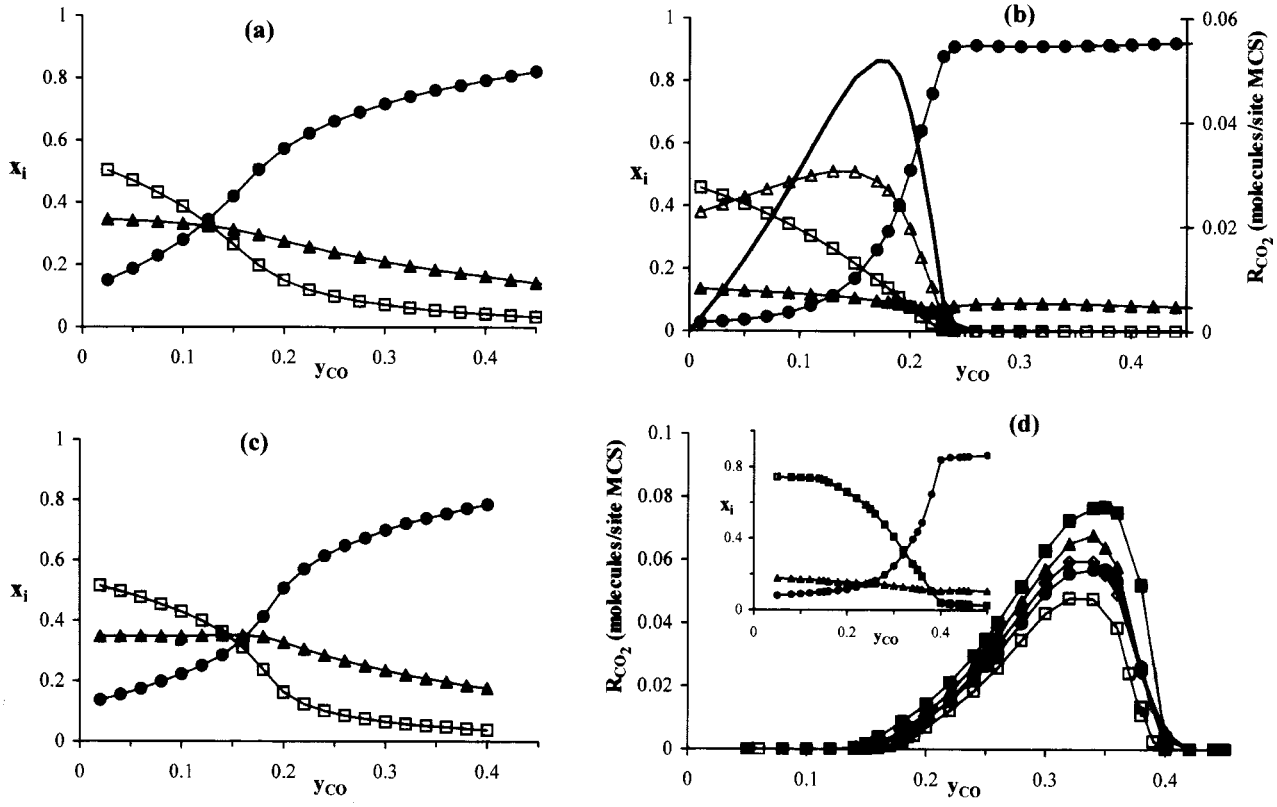


FIG. 2. The same as Fig. 1 but (a) on DLA3X for NN site coordination. (b) On DLA3X for NNN site coordination in the reactions steps, $x_E(\Delta)$. (c) On DLA3X with diffusion. (d) On FRX; production rates of $CO_2$ at different dimensions, $D$, and average number of NN adjacent sites of the fractal: ■ ($D=2.771;6.26$ NN); ▲ ($D=2.631;5.71$ NN); ◇ ($D=2.524;5.51$ NN); ● ($D=2.402;5.32$ NN); □ ($D=2.262;4.79$ NN); the phase diagram is shown in the inset.

If we overdo our semantics, we can call ''crystalline fractals'' all those two-dimensional substrates restricted to a regular square crystalline reference lattice on which fractals such as the IPC, backbone, and DLA(2D) are constructed. The checkerboard argument of BZ can then be easily extended to all two-dimensional crystalline substrates, thereby explaining the unreactivity of the system on them, even if the desorption of CO($a$) [Figs. 4(a) and 4(c)] is included.

In the case of substrate FRX, the BZ argument is not valid because the position of the active sites does not have a given reference symmetry. There is a clear reactive window with a more pronounced production maximum at a greater fractal dimension, as shown in Fig. 2(d). Since the greater the fractal dimension, the greater its roughness, an improvement in catalytic activity occurs with dimension due, as explained by Park *et al.* [21], who studied the ZGB model over the same type of substrate, not to the greater surface, since activity is expressed per active site, but to the greater number of next neighbors around the sites located in more corrugated surface regions compared to smoother ones. This promotes the landing probability of NO, through step (2) of the mechanism, and offers a better chance for the adsorbed reactant species to encounter a reacting partner. The caption of Fig. 2(d) gives the dimensions of the substrate in each case, together with the corresponding average number of adjacent sites.

The poisoning situation can be modified, for instance, by altering the degrees of freedom of the system, by allowing diagonal actions, increasing the coordination number of the active site by the participation of the next-nearest-neighbor sites (NNN) in the reaction step, but allowing dissociation to occur considering only NN sites. This situation is represented in Figs. 1(d) and 2(b) for the DLA(2D) and DLA3X substrates, respectively. The reactive window produced in these cases starts at a critical value $y_{CO(1)}=0$ in both substrates. The effect of the NNN sites was studied earlier by our group in the case of uniform two-dimensional lattices for the CO-$O_2$ [32] and CO-NO [29] reactions, and it is of practical interest to observe the general complexity of real systems in relation to the coordination of the active site in catalysts that may be formed by supported metallic particles where the surfaces are mixtures of various crystal faces.

The mechanism of the ZGB model includes, together with steps (1) and (3) above, the dissociation of $O_2$ in a manner similar to step (2), and the checkerboard argument is not applicable, so it is expected to find a reactive window. Figure 3(a) shows this model on the DLA3X substrate, and in Fig. 3(b) the diagonal actions have also been included for the reaction step. In the first case a narrow reactive window is seen between the critical concentrations 0.26 and 0.39, approximately, while in the case of diagonal actions the window goes from the origin $y_{CO(1)}=0$ to the critical transition $y_{CO(2)}$ of the window, approximately equal to that of the previous case. Moreover, both irreversible phase transitions are either continuous or second order.

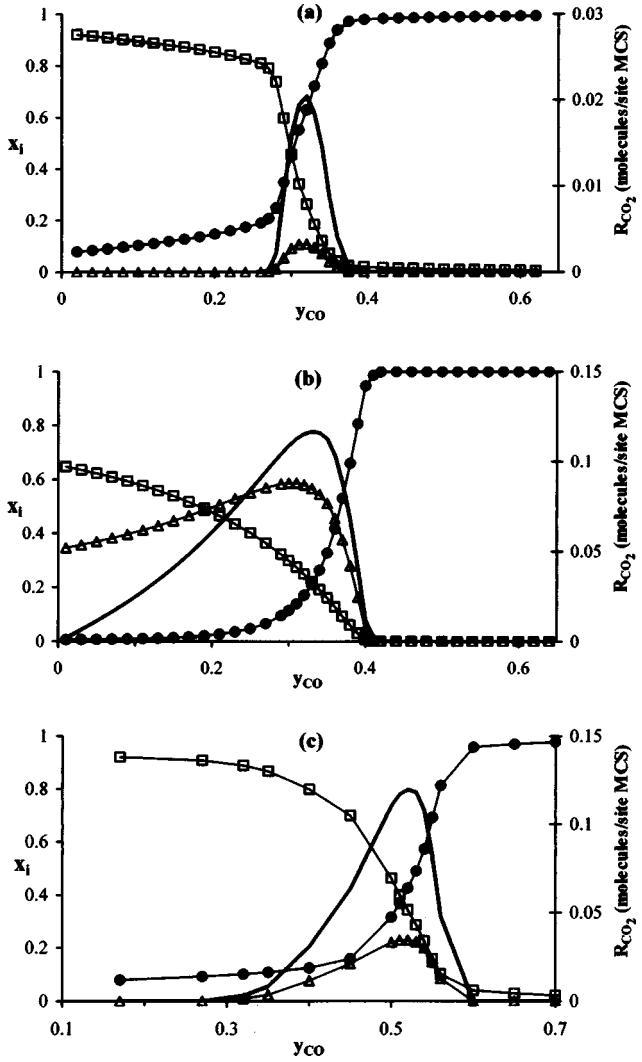


FIG. 3. Phase diagram and production rates of $CO_2$ obtained by MC for the ZGB model; $x_{CO}$ (●), $x_O$ (□), $x_E$ (Δ), production rate $R_{CO_2}$ (——). (a) On DLA3X for NN site coordination. (b) On DLA3X for NNN site coordination in the reaction steps. (c) On FRX for dimension=2.771.

Some characteristics of the ZGB model in the three-dimensional substrates are of special interest. In the case of a two-dimensional uniform or fractal surface such as the IPC or DLA(2D), all the active sites of the substrate are connected so that, since the reaction rate is infinite, CO($a$) and O($a$) cannot coexist outside the reactive window. In the three-dimensional substrates that we are considering, however, degenerate absorbent zones are seen in the region of low CO concentration consisting of either CO($a$) or O($a$), showing that the substrate has regions that are disconnected from one another. This happens, for example, in the DLA3X substrate because even though the DLA(3D) fractal that serves as its base is completely connected, the outer faces, which make up the DLA3X substrate, constitute regions that have no connections with one another. However, the introduction of diagonal actions leads to the connection of all the sites of the substrate. In the region of high CO concentration where the surface is poisoned with CO($a$), the systems with and without diagonals behave similarly. Naturally, maximum production is much higher when diagonal actions are allowed.

In Fig. 3(c) we have added the phase diagrams with the corresponding production of the ZGB model on solid FRX, which was recently studied by Park *et al.* [21,22], to show that a situation similar to that discussed in the previous paragraph with DLA3X occurs. This indicates that the deterministic fractal FRX, because of the way in which the neighbors of the active site are defined, has regions disconnected from one another that can be poisoned independently with CO($a$) or O($a$). This reminds one that a similar phenomenon occurs with the globules of the IPC fractal structure, although in that case these sectors are connected by links that retain the system's reactivity.

The effect of introducing the adsorbate's desorption steps is interesting because it corresponds to many of the situations seen in actual experience. The addition of this step is another way of producing a reactive window in the DLA3X substrate as shown in the production diagrams of Fig. 4(b) for $A/D$ ratios between 99/1 and 1/9. It is seen that the windows go up to $y_{CO}=1$. The production is expressed by site and MCS devoted only to the adsorption step. Maximum production increases with the magnitude of the desorption, since the vacant sites left by the CO($a$) molecules leaving the surface allow the appearance of empty NN pairs for the dissociative adsorption of NO. Figure 4(d) is a logarithmic diagram showing maximum production against the probability of desorption $p_d$, with a linearity that points to a scaling in which maximum production is proportional to $p_d^x$, with a value of $x$ equal to 0.80. It is also seen that maximum production shows excellent linearity with $y_{CO}$(max) concentration. No critical value was found for the desorption probability.

In the case of the ''crystalline'' two-dimensional substrates DLA(2D) and IPC, a stationary reactive pseudowindow caused by the effect of the CO desorption step seems to persist up to very high values of the number of MC iterations, as shown in Figs. 4(a) and 4(c), which correspond to 50 million MCSs devoted only to the adsorption step. It is also possible to see a pseudoscaling in the same way as with substrate DLA3X, with values of $x$ equal to 0.70 for DLA(2D) and 0.62 for the IPC. However, no linearity between maximum production and $y_{CO}$(max) as in DLA3X is seen. But in view of the ''crystallinity,'' the BZ checkerboard argument [10,11] is still valid, so these situations correspond to a ''quasisteady state'' that is poisoned slowly. In the case of the original BZ model on a uniform substrate, it has been suggested [10] that many nonreactive states can exist made of various surface regions, each with its ''black'' sites or its ''white'' sites occupied by N($a$). These phases would never be in contact with one another, since they are separated by dislocations that are occupied by either O($a$) or CO($a$). This analysis can be applied to our systems formed by ''crystalline'' substrates which also include the CO($a$) desorption step, but in this case the dislocations that separate the absorbent sectors are occupied only by O($a$). In the zone of low CO concentration there is faster poisoning of the surface, leading to out-of-phase absorbent zones of the checkerboard type separated by small O($a$) phases. On the other hand, in the high CO concentration zone the phase separation occurs

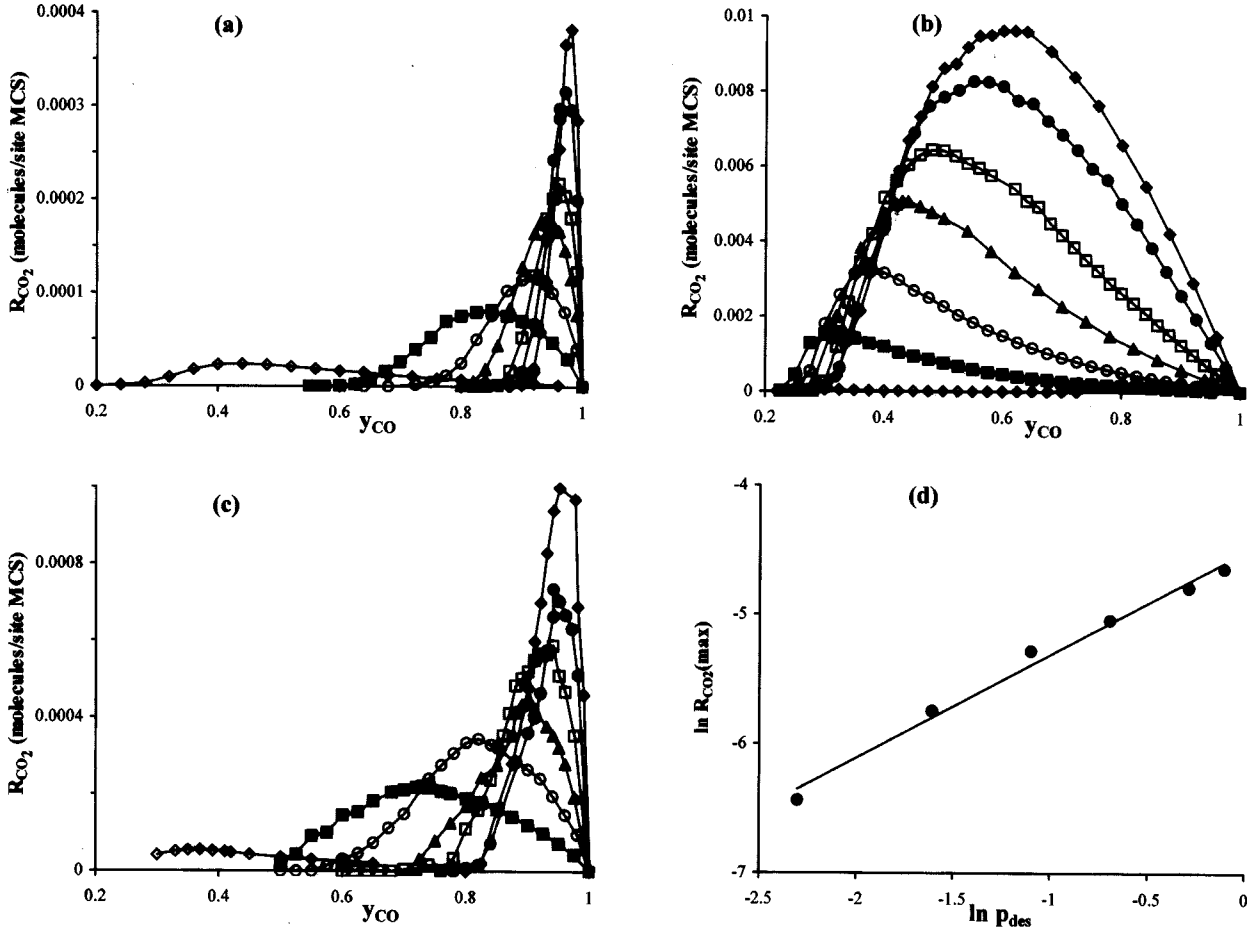


FIG. 4. The same reaction and mechanism as Fig. 1, but (a) production rate, $R_{CO_2}$, on DLA (2D) with desorption $(A/D)=$ ♦, 1/9; ●, 1/4; □, 1/1; ▲, 2/1; ○, 4/1; ■, 9/1; ◇, 99/1. (b) The same as (a) on DLA3X. (c) The same as (a) on IPC. (d) Logarithmic diagram of maximum production, $R_{CO_2}$, vs probability of desorption $p_{des}$ for the curves of (b).

also in regions made of CO($a$) and empty sites, which sometimes take a very long time, of the order of 1 to 3 million MCSs, to become poisoned, while in the homogeneous case the time is very much lower. The above explains, as seen in Figs. 4(a) and 4(c), that the pseudoreactive windows go from $y_{CO}$ values greater than zero to $y_{CO}=1$.

Finally, Table I has been introduced to provide an overall view of the different systems and situations studied in the paper in relation to the reactivity of the various processes studied.

## ACKNOWLEGMENT

The authors thank Fondecyt for financial support of this work.

## APPENDIX

### 1. Two-dimensional substrates

In the Monte Carlo program, three two-dimensional substrates were generated: the incipient percolation cluster (IPC), the IPC backbone, and the diffusion-limited aggregation (DLA) cluster fractals. They were all constructed on a two-dimensional crystalline square lattice of size $L\times L$ ($L=100$ for the IPC and 200 for the backbone) and the points generated are the active sites of the substrate that act as catalysts for the superficial reaction.

In the case of the IPC, as explained in previous papers [18], the substrate was generated by randomly blocking a fraction equal to 0.4072 of the lattice sites, considering then as active sites only those of the spanning cluster of the remaining sites computed by Hosken-Kopelman's algorithm [33], which make up the IPC, a fractal whose dimension is equal to 91/48.

In the case of the backbone, after generating the IPC, all those sites belonging to the hanging zones [30,33] are excluded using Herrmann's algorithm [31]. In this way a well characterized fractal is obtained whose dimension is equal to 1.6432.

In the case of the DLA(2D), a 10 000-element substrate was constructed as usual, fixing a seed particle on a central lattice site and adding particles, one at a time, to a growing cluster (the fractal DLA) via random-walk trajectories from a random position far from the seed. Using a criterion similar to that proposed by Meakin *et al.* [34], the random walk of the particle starts at a point on a circumference of radius $R_1$ with its center at the seed. This point is defined by randomly determining the angle $\varphi$ corresponding to polar coordinates

TABLE I. Summary of reactivities and reactive windows for various substrates and situations considered in the paper. Figures 1, 2, and 4, CO-NO reaction; Fig. 3, CO-$O_2$ reaction and ZGB model. *R*, reactive, NR, nonreactive.

| Substrate | Reactivity (reactive window) | Figure |
|---|---|---|
| Uniform (2D) | NR | 1(a) |
| IPC (2D) | NR | 1(b) |
| Backbone (2D) | NR | |
| DLA (2D) (NN) | NR | 1(c) |
| DLA 2D (NNN) | $R$ $(y_1=0.02, y_2=0.22)$ | 1(d) |
| DLA3X (NN) | NR | 2(a) |
| DLA3X (NNN) | $R$ $(y_1=0, y_2=0.24)$ | 2(b) |
| DLA3X (diffusion) | NR | 2(c) |
| FRX ($D=2.771-2.262$) | $R$ $(y_1=0.14, y_2=0.4)$ | 2(d) |
| DLA3X (ZGB) (NN) | $R$ $(y_1=0.26, y_2=0.38)$ | 3(a) |
| DLA3X (ZGB) (NNN) | $R$ $(y_1=0, y_2=0.41)$ | 3(b) |
| FRX ($D=2.771$) (ZGB) | $R$ $(y_1=0.17, y_2=0.56)$ | 3(c) |
| DLA (2D) (desorption) | NR (quasireactivity) | 4(a) |
| DLA3X (desorption) | $R$ $(y_1=0.3, y_2=1)$ $A/D=1/9$ | 4(b) |
| | $R$ $(y_1=0.28, y_2=1)$ $A/D=2/1$ | 4(b) |
| IPC (desorption) | NR | |

whose origin is at the seed. The random walk continues until the particle is added to the cluster (when it goes by an NN site of some cluster element) or until it goes outside the limits of a new circle of radius $R_2 > R_1$ concentric with $R_1$, and then a new attempt is started. If the distance between the particle of the cluster farthest from the center and the circumference of radius $R_1$ is smaller than a certain amount, the values of $R_1$ and $R_2$ are increased. The DLA(2D) substrate built in this way consists of a 2D fractal of dimension $D = 1.68$.

Since all the above fractals are probabilistic or nondeterministic, it was necessary to generate a large number of them, so that the properties obtained from MC for the CO-NO reaction are the average of the results of the simulations carried out on those substrates.

#### 2. Three-dimensional substrates

Two three-dimensional catalytic substrates were used in the simulations. In the first one, which we have called DLA3X, the outer surface of a statistical DLA fractal built on a three- dimensional cubic lattice was considered. In the second case the active sites were the points generated in the three-dimensional space from a series of affine transformations, thereby giving rise to the generation of deterministic fractals that we have called FRX.

To build the first of these substrates we first generated a three-dimensional diffusion-limited aggregation DLA(3D) of 2000 elements on a cubic lattice, which is its support, by a procedure that is essentially the same as the one described for the DLA(2D). The starting sites in the two- dimensional case were set by randomly choosing an angle, while in the three-dimensional case we consider randomly $z$ and the angle in cylindrical coordinates. The substrate, which we have called DLA3X, assumes that each of the active sites is located on one of the exposed outer faces of the cubes which make up the elements of the three-dimensional DLA(3D) fractal. This means that the DLA3X substrate is a reproducible disordered surface, constructed on a fractal, but is not strictly a fractal.

The FRX substrates were obtained by generating a series of deterministic fractals of different dimensions based on a symmetry theoretical concept of fractal geometry [35] in the same way as the surfaces used by Park *et al.* [21,22] in MC studies of catalytic CO oxidation. The method consists in the construction of multifractal surfaces by the repetition of self-similar structures within a structure at successively finer length scales, assigning a set of affine transformations $\{\omega_i\}$ which contract and move the structure, such that the union of these images constitutes the given fractal itself, i.e.,

$$X = \bigcup_{i=1}^{n} \omega_i(X), \tag{A1}$$

where $X$ is the fractal and $n$ is the number of associated affine transformations [35]. If $\lambda_i$ is the scaling factor of the $i$th affine transformation, $\omega_i$, it is possible to determine the dimension $D$ of the fractal from the relation

$$\sum_{i=1}^{n} \lambda_i^D = 1. \tag{A2}$$

In our work we consider a fractal support defined by sets of affine transformations of the form

$$\omega_i \begin{pmatrix} x \\ y \\ x \end{pmatrix} = \lambda_i \begin{pmatrix} \cos\theta_i & -\sin\theta_i & 0 \\ \sin\theta_i & \cos\theta_i & 0 \\ 0 & 0 & 1 \end{pmatrix} \begin{pmatrix} x \\ y \\ z \end{pmatrix} + \begin{pmatrix} l_i \\ m_i \\ n_i \end{pmatrix} \tag{A3}$$

considering the scaling factor $\lambda_i$ equal to 1/3 in all of them. The values of the rotational angles $\theta_i$ and the translations $l_i$, $m_i$, and $n_i$ in the respective $x$, $y$, and $z$ directions were those

given in Table I of Ref. [21]. In general, fractals of different dimension can be obtained by changing the number of affine transformations and the associated scaling factors.

To construct the fractals on the computer, use was made of the random iteration algorithm [21,22] as follows: a sequence of spatial points $\{\mathbf{r}_N : N=0,1,2,\ldots\}$ is generated recursively by applying the transformation

$$\mathbf{r}_N = \omega_i(\mathbf{r}_{N-1}) \tag{A4}$$

from any point $\mathbf{r}_0$ in space, e.g., the origin. At each step, a particular transformation, say $\omega_i$, is selected with an assigned probability $p_i$ from an arbitrary set $\{p_i\}$ such that $\Sigma_i p_i = 1$. In our case, 4000 points were generated in this way, becoming the active sites of the FRX substrates. Neighbors of a site of the FRX fractal are considered to be all those fractal sites located in a spherical environment of radius $R$, determined, following Park *et al.* [21,22], as twice the average distance between every surface site and its nearest neighbor.


[1] G. Nicolis and I. Prigogine, *Self-Organization in Nonequilibrium Systems* (Wiley Interscience, New York, 1977); H. Haken, *Synergetics* (Springer-Verlag, New York, 1977); J. Marro and R. Dickman, *Nonequilibrium Phase Transitions in Lattice Models* (Cambridge University Press, Cambridge, 1999).

[2] J. W. Evans, Langmuir **7**, 2514 (1991).

[3] V. P. Zhdanov and B. Kasemo, Surf. Sci. Rep. **20**, 111 (1994).

[4] E. V. Albano, Heterog. Chem. Rev. **3**, 389 (1996); E. V. Albano in M. Borówko, *Computational Methods in Surface and Colloid Science* (Marcel Dekker, New York, 2000), Chap. 8, pp. 387–437.

[5] R. M. Ziff, E. Gulari, and Y. Barshad, Phys. Rev. Lett. **56**, 2553 (1986).

[6] K. Fichthorn, E. Gulari, and R. Ziff, Phys. Rev. Lett. **63**, 1527 (1989); Eng. Sci. **44**, 1403 (1989); E. Albano, Phys. Rev. A **46**, 5020 (1992).

[7] K. M. Khan, K. Yaldram, and N. Ahmad, J. Chem. Phys. **109**, 5054 (1998).

[8] K. M. Khan, K. Yaldram, N. Ahmad, and Qamar-ul-Haque, Physica A **268**, 89 (1999); K. M. Khan, A. Basit, and K. Yaldram, J. Phys. A **33**, L215 (2000).

[9] D. ben-Avraham and J. Kohler, J. Stat. Phys. **65**, 839 (1991).

[10] B. J. Brosilow and R. M. Ziff, J. Catal. **136**, 275 (1992).

[11] B. Meng, W. H. Weinberg, and J. W. Evans, Phys. Rev. E **48**, 3577 (1993).

[12] K. Yaldram and M. A. Khan, J. Catal. **131**, 369 (1991).

[13] J. Cortés, H. Puschmann, and E. Valencia, J. Chem. Phys. **105**, 6026 (1996); **109**, 6086 (1998).

[14] A. Dickman, B. C. Grandi, W. Figueiredo, and R. Dickman, Phys. Rev. E **59**, 6361 (1999).

[15] E. V. Albano, Phys. Rev. B **42**, 10 818 (1990); Surf. Sci. **235**, 351 (1990); Phys. Rev. A **46**, 5020 (1992).

[16] A. Casties, J. Mai, and W. von Niessen, J. Chem. Phys. **99**, 3082 (1993).

[17] J. P. Hovi, J. Vaari, H. P. Kaukonen, and R. M. Nieminen, Comput. Mater. Sci. **1**, 33 (1992).

[18] E. Valencia and J. Cortés, Surf. Sci. **470**, L109 (2000); J. Cortés and E. Valencia, Physica A **309**, 26 (2002).

[19] J. Mai, A. Casties, and W. von Niessen, Chem. Phys. Lett. **211**, 197 (1993).

[20] J. Mai, A. Casties, and W. von Niessen, Chem. Phys. Lett. **196**, 358 (1992); A. Tretyakov and H. Takayasu, Phys. Rev. A **44**, 8388 (1991); Zhuo Gao and R. Yang, Phys. Rev. E **60**, 2741 (1999); I. Jensen, J. Phys. A **24**, L111 (1991).

[21] H. Park, H. Kim, and S. Lee, Surf. Sci. **380**, 514 (1997).

[22] H. Park and S. Lee, Surf. Sci. **411**, 1 (1998).

[23] X.-Y. Guo and J. Keil, Chem. Phys. Lett. **330**, 410 (2000).

[24] K. C. Taylor, Catal. Rev. Sci. Eng. **35**, 457 (1993); M. Shelef and G. Graham, *ibid.* **36**, 433 (1994); S. Oh, G. Fischer, J. Carpenter, and D. Goodman, J. Catal. **100**, 360 (1986); B. K. Cho, *ibid.* **148**, 697 (1994); **162**, 149 (1996); D. N. Belton, C. L. Di, Maggio, S. J. Schmieg, and K. Y. Simon, *ibid.* **157**, 559 (1995); Ch. H. F. Peden, D. N. Belton, and S. J. Schmieg, *ibid.* **155**, 204 (1995).

[25] S. Chuang and C. Tan, J. Catal. **173**, 95 (1998).

[26] P. Araya, F. Gracia, J. Cortés, and E. Wolf, Appl. Catal., B **997**, 1 (2002).

[27] M. A. Khan, K. Yaldram, G. K. Khalil, and K. M. Khan, Phys. Rev. E **50**, 2156 (1994).

[28] B. Meng, W. H. Weinberg, and J. W. Evans, J. Chem. Phys. **101**, 3234 (1994).

[29] J. Cortés and E. Valencia, Chem. Phys. **229**, 265 (1998).

[30] D. Stauffer and A. Aharony, *Introduction to Percolation Theory*, 2nd ed. (Taylor and Francis, London, 1992).

[31] H. J. Herrmann and H. E. Stanley, Phys. Rev. Lett. **53**, 1121 (1984); H. J. Herrmann, D. Hong, and H. E. Stanley, J. Phys. A **17**, L261 (1984).

[32] J. Cortés and E. Valencia, Surf. Sci. **371**, L243 (1997); J. Cortés, E. Valencia, and H. Puschmann, Phys. Chem. Chem. Phys. **1**, 1577 (1999).

[33] J. Hoshen and R. Kopelman, Phys. Rev. B **14**, 3438 (1976); R. Kopelman, J. Stat. Phys. **42**, 185 (1986).

[34] P. Meakin, R. C. Ball, P. Ramanlal, and L. M. Sander, Phys. Rev. A **35**, 5233 (1987); S. Tolman and P. Meakin, *ibid.* **40**, 428 (1989).

[35] M. F. Barnsley, *Fractals Everywhere* (Academic, New York, 1988); M. Barnsley, in Proc. Symposia in Applied Mathematics, edited by R. L. Devaney and L. Keen (American Mathematical Society, Providence, 1988), Vol. 39.